

Metallacycles of Iron, Zinc, and Cadmium Assembled by Polytopic Bis(pyrazolyl)methane Ligands and Fluoride Abstraction from BF_4^-

Daniel L. Reger,* Russell P. Watson, James R. Gardinier,† Mark D. Smith, and Perry J. Pellechia

Department of Chemistry and Biochemistry, University of South Carolina, Columbia, South Carolina 29208

Received July 16, 2006

Reactions of the arene-linked bis(pyrazolyl)methane ligands *m*-bis[bis(1-pyrazolyl)methyl]benzene (*m*-[CH(pz)₂]₂C₆H₄, **L_m**) and 1,3,5-tris[bis(1-pyrazolyl)methyl]benzene (1,3,5-[CH(pz)₂]₃C₆H₃, **L³**) with BF_4^- salts of divalent iron, zinc, and cadmium result in fluoride abstraction from BF_4^- and formation of fluoride-bridged metallacyclic complexes. Treatment of $\text{Fe}(\text{BF}_4)_2 \cdot 6\text{H}_2\text{O}$ and $\text{Zn}(\text{BF}_4)_2 \cdot 5\text{H}_2\text{O}$ with **L_m** leads to the complexes $[\text{Fe}_2(\mu\text{-F})(\mu\text{-L}_m)_2](\text{BF}_4)_3$ (**1**) and $[\text{Zn}_2(\mu\text{-F})(\mu\text{-L}_m)_2](\text{BF}_4)_3$ (**2**), in which a single fluoride ligand and two **L_m** molecules bridge the two metal centers. The reaction of $[\text{Cd}_2(\text{thf})_5](\text{BF}_4)_4$ with **L_m** results in the complex $[\text{Cd}_2(\mu\text{-F})_2(\mu\text{-L}_m)_2](\text{BF}_4)_2$ (**3**), which contains dimeric cations in which two fluoride and two **L_m** ligands bridge the cadmium centers. Equimolar amounts of the tritopic ligand **L³** and $\text{Zn}(\text{BF}_4)_2 \cdot 5\text{H}_2\text{O}$ react to give the related monofluoride-bridged complex $[\text{Zn}_2(\mu\text{-F})(\mu\text{-L}^3)_2](\text{BF}_4)_3$ (**4**), in which one bis(pyrazolyl)methane unit on each ligand remains unbound. NMR spectroscopic studies show that in acetonitrile the zinc metallacycles observed in the solid-state remain intact in solution.

Introduction

The occurrence of metal–fluoride fragments in transition metal-mediated C–F bond activation reactions has spurred research into discrete metal–fluoride compounds.^{1,2} Current research in this area has led to fundamental advances further demonstrating, for example, that compounds can be isolated in which the hard fluoride anion acts as a viable ligand toward soft, low-valent transition metal cations.³

One of the largest hurdles for the research into transition metal fluorides is the intentional synthesis of well-behaved, soluble complexes.^{2,4} Recent work by Holland,⁵ among others,⁴ has demonstrated the feasibility of a controlled synthetic approach using convenient fluorinating reagents. The isolation of fluoride-containing transition metal complexes, however, has often relied on the serendipitous decomposition of fluoride-containing compounds.^{4,6} The decomposition of the tetrafluoroborate anion, through hydrolysis or fluoride abstraction, has long been known as a potential fluoride source in coordination compounds.⁷ As an example related to the results presented here, although crystallographic confirmation of the structures was not obtained, Reedijk reported thorough characterization of the bis(pyrazolyl)methane ligand-supported fluoride-bridged complexes $[\text{M}_2(\text{dmpm})_4(\mu\text{-F})_2]\text{X}_2$ (dmpm = bis(3,5-dimethylpyrazol-1-yl)methane; M = Fe, Co, Ni, Cd, or Mn; X = BF_4^- or ClO_4^-) formed from BF_4^- decomposition.⁸

* To whom correspondence should be addressed. E-mail: reger@mail.chem.sc.edu.

† Present address: Department of Chemistry, Marquette University, Milwaukee, WI 53201-1881.

- (1) (a) Kiplinger, J. L.; Richmond, T. G.; Osterberg, C. E. *Chem. Rev.* **1994**, *94*, 373. (b) Jasim, N. A.; Perutz, R. N.; Whitwood, A. C.; Braun, T.; Izundu, J.; Neumann, B.; Rothfield, S.; Stammer, H.-G. *Organometallics* **2004**, *23*, 6140. (c) Cronin, L.; Higgitt, C. L.; Karch, R.; Perutz, R. N. *Organometallics* **1997**, *16*, 4920. (d) Bennett, B. K.; Harrison, R. G.; Richmond, T. G. *J. Am. Chem. Soc.* **1994**, *116*, 11165. (e) Ferrando-Miguel, G.; Gérard, H.; Eisenstein, O.; Caulton, K. G. *Inorg. Chem.* **2002**, *41*, 6440. (f) Kraft, B. M.; Lachicotte, R. J.; Jones, W. D. *J. Am. Chem. Soc.* **2001**, *123*, 10973. (g) Verdagner, X.; Lange, U. E. W.; Reding, M. T.; Buchwald, S. L. *J. Am. Chem. Soc.* **1996**, *118*, 6784. (h) Grushin, V. V.; Marshall, W. J. *J. Am. Chem. Soc.* **2004**, *126*, 3068. (i) Braun, T.; Noveski, D.; Neumann, B.; Stammer, H.-G. *Angew. Chem., Int. Ed.* **2002**, *41*, 2745.
- (2) (a) Kirkham, M. S.; Mahon, M. F.; Whittlesey, M. K. *Chem. Commun.* **2001**, 813. (b) Grushin, V. V. *Chem.—Eur. J.* **2002**, *8*, 1006. (c) Noveski, D.; Braun, T.; Schulte, M.; Neumann, B.; Stammer, H.-G. *Dalton Trans.* **2003**, 4075.
- (3) Doherty, N. M.; Hoffman, N. W. *Chem. Rev.* **1991**, *91*, 553.

- (4) Murphy, E. F.; Murugavel, R.; Roesky, H. W. *Chem. Rev.* **1997**, *97*, 3425.
- (5) Vela, J.; Smith, J. M.; Yu, Y.; Ketterer, N. A.; Flaschenriem, C. J.; Lachicotte, R. J.; Holland, P. L. *J. Am. Chem. Soc.* **2005**, *127*, 7857.
- (6) Crabtree, R. H.; Hlatky, G. G.; Holt, E. M. *J. Am. Chem. Soc.* **1983**, *105*, 7302.
- (7) Reedijk, J. *Comments Inorg. Chem.* **1982**, *1*, 379.
- (8) Verbiest, J.; van Ooijen, J. A. C.; Reedijk, J. *J. Inorg. Nucl. Chem.* **1980**, *42*, 971.

Intentional and controlled decomposition of BF_4^- can be a useful method of delivering F^- , particularly in solvents that do not dissolve binary metal fluorides⁸ but do dissolve the BF_4^- salts of the same metals.^{7–9} Furthermore, using BF_4^- salts of the metals of interest eliminates the need to add a separate fluorinating agent and to later remove the resulting byproduct. Given the above observations and our interest in the design of multitopic, third-generation poly-(pyrazolyl)methane ligands (third-generation scorpionate ligands are specifically functionalized at the noncoordinating, “back” position),^{10,11} including bitopic ligands linked by a variety of organic spacers,¹² we were intrigued by the possibility of preparing ligands for the cooperative activation of the BF_4^- anion by dinuclear Lewis acid fragments as in Figure 1. Coordination of fluorinated anions to one or more metal centers in a fashion similar to that proposed in Figure 1 is often observed in synthetically useful reactive complex precursors.¹³ Furthermore, bimetallic complexes such as those

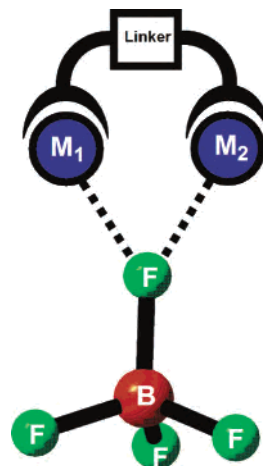


Figure 1. Proposed double activation of the tetrafluoroborate anion promoted by potentially dinucleating “third-generation” (linked) poly-(pyrazolyl)methanes.

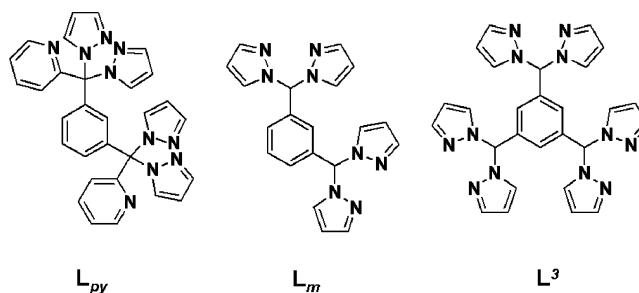


Figure 2. Examples of polytopic bis(pyrazolyl)methane ligands.

- (9) (a) van Albada, G. A.; Roubeau, O.; Mutikainen, I.; Turpeinen, U.; Reedijk, J. *New J. Chem.* **2003**, *27*, 1693. (b) Rietmeijer, F. J.; van Albada, G. A.; de Graaff, R. A. G.; Haasnoot, J. G.; Reedijk, J. *Inorg. Chem.* **1985**, *24*, 3597. (c) Rietmeijer, F. J.; de Graaff, R. A. G.; Reedijk, J. *Inorg. Chem.* **1984**, *23*, 151. (d) Vreugdenhil, W.; Birker, P. J. M. W. L.; ten Hoedt, R. W. M.; Verschoor, G. C.; Reedijk, J. *J. Chem. Soc., Dalton Trans.* **1984**, 429. (e) Keij, F. S.; de Graaff, R. A. G.; Haasnoot, J. G.; de Graaff, R. A. G.; Oosterling, A. J.; Pedersen, Erik; Reedijk, J. *J. Chem. Soc., Chem. Commun.* **1988**, 423. (f) Casellas, H.; Pevec, A.; Kozlevčar, Gamez, P.; Reedijk, J. *Polyhedron* **2005**, *24*, 1549. (g) Velthuisen, W. C.; Haasnoot, J. G.; Kinneging, A. J.; Rietmeijer, F. J.; Reedijk, J. *J. Chem. Soc., Chem. Commun.* **1983**, 1366. (h) Reedijk, J.; Jansen, J. C.; van Koningsveld, H.; van Kralingen, C. G. *Inorg. Chem.* **1978**, *17*, 1990. (i) Ackermann, J.; Meyer, F.; Pritzkow, H. *Inorg. Chem. Acta* **2004**, *357*, 3703.
- (10) Trofimenko, S. *Scorpionates: The Coordination Chemistry of Polypyrazolylborate Ligands*; Imperial College, London, 1999.
- (11) (a) White, D.; Faller, J. W. *J. Am. Chem. Soc.* **1982**, *104*, 1548. (b) Reger, D. L.; Gardinier, J. R.; Gemmill, W. R.; Smith, M. D.; Shahin, A. M.; Long, G. J.; Rebbouh, L.; Grandjean, F. *J. Am. Chem. Soc.* **2005**, *127*, 2303. (c) Reger, D. L.; Gardinier, J. R.; Bakbak, S.; Semeniuc, R. F.; Bunz, U. H. F.; Smith, M. D. *New J. Chem.* **2005**, *29*, 1035. (d) Brock, C. P.; Das, M. K.; Minton, R. P.; Niedenzu, K. *J. Am. Chem. Soc.* **1988**, *110*, 817. (e) Janiak, C.; Braun, L.; Girgsdies, F. *J. Chem. Soc., Dalton Trans.* **1999**, 3133. (f) Kisko, J. L.; Hascall, T.; Kimblin, C.; Parkin, G. *J. Chem. Soc., Dalton Trans.* **1999**, 1929. (g) Hardin, N. C.; Jeffrey, J. C.; McCleverty, J. A.; Rees, L. H.; Ward, M. A. *New J. Chem.* **1998**, *22*, 661. (h) Niedenzu, K.; Trofimenko, S. *Inorg. Chem.* **1985**, *24*, 4222. (i) Jäkle, F.; Polborn, K.; Wagner, M. *Chem. Ber.* **1996**, *129*, 603. (j) Fabrizi de Biani, F.; Jäkle, F.; Spiegler, M.; Wagner, M.; Zanello, P. *Inorg. Chem.* **1997**, *36*, 2103. (k) Herdtweck, E.; Peters, F.; Scherer, W.; Wagner, M. *Polyhedron* **1998**, *17*, 1149. (l) Guo, S. L.; Peters, F.; Fabrizi de Biani, F.; Bats, J. W.; Herdtweck, E.; Zanello, P.; Wagner, M. *Inorg. Chem.* **2001**, *40*, 4928. (m) Guo, S. L.; Bats, J. W.; Bolte, M.; Wagner, M. *J. Chem. Soc., Dalton Trans.* **2001**, 3572. (n) Bieller, S.; Zhang, F.; Bolte, M.; Bats, J. W.; Lerner, H.-W.; Wagner, M. *Organometallics* **2004**, *23*, 2107.
- (12) (a) Reger, D. L.; Gardinier, J. R.; Semeniuc, R. F.; Smith, M. D. *J. Chem. Soc., Dalton Trans.* **2003**, 1712. (b) Reger, D. L.; Watson, R. P.; Gardinier, J. R.; Smith, M. D. *Inorg. Chem.* **2004**, *43*, 6609. (c) Reger, D. L.; Gardinier, J. R.; Grattan, T. C.; Smith, M. R.; Smith, M. D. *New J. Chem.* **2003**, *27*, 1670. (d) Reger, D. L.; Semeniuc, R. F.; Smith, M. D. *J. Organomet. Chem.* **2003**, *666*, 87. (e) Reger, D. L.; Brown, K. J.; Smith, M. D. *J. Organomet. Chem.* **2002**, *658*, 50. (f) Reger, D. L.; Wright, T. D.; Semeniuc, R. F.; Grattan, T. C.; Smith, M. D. *Inorg. Chem.* **2001**, *40*, 6212. (g) Reger, D. L.; Semeniuc, R. F.; Smith, M. D. *Inorg. Chem.* **2003**, *42*, 8137. (h) Reger, D. L.; Brown, K. J.; Gardinier, J. R.; Smith, M. D. *Organometallics* **2003**, *22*, 4973. (i) Reger, D. L.; Watson, R. P.; Smith, M. D.; Pellechia, P. J. *Organometallics* **2005**, *24*, 1544. (j) Reger, D. L.; Gardinier, J. R.; Smith, M. D. *Polyhedron* **2004**, *23*, 291. (k) Reger, D. L.; Watson, R. P.; Smith, M. D.; Pellechia, P. J. *Organometallics* **2006**, *25*, 743.
- (13) (a) Beck, W.; Stünkel, K. *Chem. Rev.* **1988**, *88*, 1405. (b) Hitchcock, P. B.; Lappert, M. F.; Taylor, R. G. *J. Chem. Soc., Chem. Commun.* **1984**, 1082.

generalized in Figure 1 have received considerable attention as biomimetic catalysts for the cooperative cleavage or hydrolysis of biologically important molecules such as RNA and phosphate esters.¹⁴

We were therefore encouraged by the results we obtained with the linked heteroscorpionate ligand m -[C(py)(pz)₂]₂C₆H₄ (Figure 2; py = 2-pyridyl; pz = 1-pyrazolyl),^{12j} whose iron(II) tetrafluoroborate complex afforded a proof-of-concept that the juxtaposition of highly Lewis acidic centers could mediate fluoride abstraction and yield unusual fluoride-bridged structures, as shown by the ORTEP drawing in Figure 3 (see also the Supporting Information). Unfortunately, the exceedingly low solubility of this compound, presumably due to extensive noncovalent interactions, proved detrimental to its full characterization. We reasoned that more soluble derivatives might be prepared in higher yields from analogous ligands in which the pyridyl groups were replaced by hydrogen atoms. Herein, we describe the reactions of the ligand m -[CH(pz)₂]₂C₆H₄ (L_m , Figure 2),¹²ⁱ a direct analogue to L_{py} , with BF_4^- salts of some divalent metals (Fe, Zn, Cd) to demonstrate the generality of the fluoride abstraction. We also report the reaction of the related, mesitylene-based ligand 1,3,5-[CH(pz)₂]₃C₆H₃ (L^3 , Figure 2)^{12k} with $\text{Zn}(\text{BF}_4)_2$ that also yields a fluoride-bridged compound.

- (14) (a) Molenveld, P.; Engbersen, J. F. J.; Reinhoudt, D. N. *Chem. Soc. Rev.* **2000**, *29*, 75. (b) Wilcox, D. E. *Chem. Rev.* **1996**, *96*, 2435. (c) Williams, N. H.; Takasaki, B.; Wall, M.; Chin, J. *Acc. Chem. Res.* **1999**, *32*, 485.

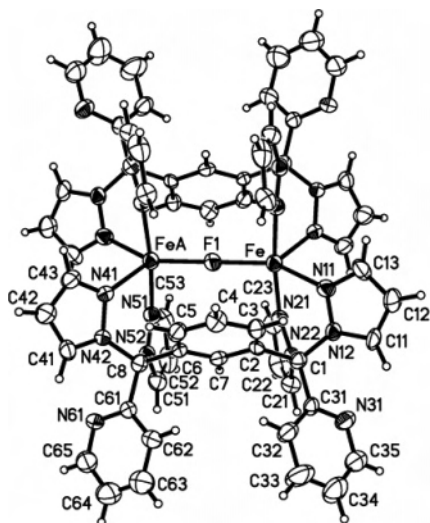


Figure 3. ORTEP representation of the cationic macrocycle in $[\text{Fe}_2(\mu\text{-F})(\mu\text{-}m\text{-}[\text{CH}(\text{pz})_2]_2\text{C}_6\text{H}_4)_2](\text{BF}_4)_3$. Displacement ellipsoids drawn at the 50% probability level. For selected bond lengths and angles, see the Supporting Information.

Experimental Section

General Considerations. Air-sensitive materials were handled under a nitrogen atmosphere using standard Schlenk techniques or in a Vacuum Atmospheres HE-493 drybox. All solvents were dried by conventional methods prior to use. The compounds $m\text{-}[\text{CH}(\text{pz})_2]_2\text{C}_6\text{H}_4$,¹²ⁱ $1,3,5\text{-}[\text{CH}(\text{pz})_2]_3\text{C}_6\text{H}_3$,^{12k} and $[\text{Cd}_2(\text{thf})_5](\text{BF}_4)_4$ ¹⁵ were prepared following reported procedures. All other chemicals were purchased from Aldrich or Fisher Scientific and used as received. Reported melting points are uncorrected. IR spectra were obtained on a Nicolet 5DXBO FTIR spectrometer. ¹H, ¹³C, and ¹⁹F NMR spectra were recorded on a Varian Mercury/VX 300, a Varian Mercury/VX 400, or a Varian INOVA 500 spectrometer. All chemical shifts are in ppm and were referenced to residual undeuterated solvent signals (¹H), deuterated solvent signals (¹³C), or externally to CFCl_3 (¹⁹F). Relaxation times were measured using the vendor-supplied CPMG pulse sequence. Mass spectrometric measurements were obtained on a MicroMass QTOF spectrometer. Elemental analyses were performed on vacuum-dried samples by Robertson Microlit Laboratories (Madison, NJ). Solution magnetic susceptibilities were determined at 295 K by the Evans Method.¹⁶

$[\text{Fe}_2(\mu\text{-F})(\mu\text{-}m\text{-}[\text{CH}(\text{pz})_2]_2\text{C}_6\text{H}_4)_2](\text{BF}_4)_3$ (1). A 10-mL THF solution of $\text{Fe}(\text{BF}_4)_2 \cdot 6\text{H}_2\text{O}$ (0.27 g, 0.80 mmol) was added by cannula to a 15-mL THF solution of $m\text{-}[\text{CH}(\text{pz})_2]_2\text{C}_6\text{H}_4$ (0.30 g, 0.81 mmol). A precipitate immediately formed, and the system developed a pale yellow color. After 8.5 h of stirring at room temperature, the precipitate was isolated by cannula filtration and washed with 10 mL of THF. Drying in vacuo overnight yielded 0.40 g (88%) of an off-white solid. Single crystals suitable for X-ray studies were grown by the vapor diffusion of Et_2O into 1-mL CH_3CN solutions of **1** and taken directly from the mother liquor as **1**·**1.5** CH_3CN . Crystals used for elemental analysis were removed from the mother liquor, rinsed with ether, and dried in vacuo, which resulted in loss of solvent of crystallization. mp > 330 °C. Anal. Calcd for $\text{C}_{40}\text{H}_{36}\text{B}_3\text{F}_{13}\text{Fe}_2\text{N}_{16}$: C, 42.44; H, 3.21; N, 19.80. Found: C, 42.93; H, 3.05; N, 19.66. IR (KBr, cm^{-1}): 3129, 2917, 1457, 1405, 1293, 1053, 774, 766, 632, 519. ¹H NMR (400 MHz, CD_3CN): δ 44.30 (s), 33.32 (s), 15.16 (s), 14.29 (s), 8.50 (br s),

−1.50 (br s), −3.43 (s), −10.51 (s), −18.40 (s). ¹⁹F NMR (376 MHz, CD_3CN): δ −151 (BF_4^-). MS ESI(+) m/z (rel. % abund.) [assign]: 883 (1) $[\text{Fe}(\text{L}_m)_2\text{BF}_4]^+$, 815 (1) $[\text{Fe}(\text{L}_m)_2\text{F}]^+$, 445 (1) $[\text{Fe}(\text{L}_m)\text{F}]^+$, 398 (20) $[\text{Fe}(\text{L}_m)_2]^{2+}$, 371 (75) $[\text{L}_m + \text{H}]^+$, 303 (100) $[\text{L}_m - \text{pz}]^+$.

$[\text{Zn}_2(\mu\text{-F})(\mu\text{-}m\text{-}[\text{CH}(\text{pz})_2]_2\text{C}_6\text{H}_4)_2](\text{BF}_4)_3$ (2). A 10-mL acetone solution of $m\text{-}[\text{CH}(\text{pz})_2]_2\text{C}_6\text{H}_4$ (0.11 g, 0.30 mmol) was added by cannula to a 10-mL acetone solution of $\text{Zn}(\text{BF}_4)_2 \cdot 5\text{H}_2\text{O}$ (0.10 g, 0.31 mmol). After 4 h of stirring at room temperature, a white precipitate had formed. This solid was isolated by cannula filtration, washed with 5 mL of acetone, and dried in vacuo to yield 0.084 g (49%) of **2**. Single crystals suitable for X-ray studies were grown by the vapor diffusion of Et_2O into 1-mL CH_3CN solutions of **2** and taken directly from the mother liquor as **2**·**1.5** CH_3CN . Crystals for elemental analysis were removed from the mother liquor, rinsed with ether, and dried in vacuo, which resulted in loss of solvent of crystallization. mp > 330 °C. Anal. Calcd for $\text{C}_{40}\text{H}_{36}\text{B}_3\text{F}_{13}\text{N}_{16}\text{Zn}_2$: C, 41.74; H, 3.15; N, 19.47. Found: C, 42.05; H, 3.04; N, 19.85. IR (KBr, cm^{-1}): 3158, 3131, 1515, 1457, 1410, 1293, 1052, 776, 523. ¹H NMR (300 MHz, CD_3CN): δ 8.39 (dd, $J = 0.6$, 2.7 Hz, 4 H, 5/3-pz), 8.16 (d, $J = 2.7$ Hz, 4 H, 5/3-pz), 8.11 (s, 4 H, $\text{CH}(\text{pz})_2$), 7.52 (t, $J = 8.0$ Hz, 2 H, C_6H_4), 7.38 (d, $J = 2.1$ Hz, 4 H, 5/3-pz), 6.63 (d, $J = 2.4$ Hz, 4 H, 5/3-pz), 6.59 (d, $J = 7.8$ Hz, 4 H, C_6H_4), 6.50 (t, $J = 2.3$ Hz, 4 H, 4-pz), 6.40 (t, $J = 2.4$ Hz, 4 H, 4-pz), 4.61 (s, 2 H, C_6H_4). ¹³C NMR (126 MHz, CD_3CN): δ 144.7, 144.1, 137.9, 137.1, 136.2, 130.4, 128.5, 125.0, 108.2 (two unresolved signals, 4-pz), 74.9. ¹⁹F NMR (376 MHz, CD_3CN): δ −150 (BF_4^-), −211 (Zn–F–Zn). MS ESI(+) m/z (rel. % abund.) [assign]: 891 (1) $[\text{Zn}(\text{L}_m)_2\text{BF}_4]^+$, 823 (1) $[\text{Zn}(\text{L}_m)_2\text{F}]^+$, 453 (5) $[\text{Zn}(\text{L}_m)\text{F}]^+$, 402 (20) $[\text{Zn}(\text{L}_m)_2]^{2+}$, 371 (60) $[\text{L}_m + \text{H}]^+$, 303 (100) $[\text{L}_m - \text{pz}]^+$.

$[\text{Cd}_2(\mu\text{-F})_2(\mu\text{-}m\text{-}[\text{CH}(\text{pz})_2]_2\text{C}_6\text{H}_4)_2](\text{BF}_4)_2$ (3). A 10-mL acetone solution of $m\text{-}[\text{CH}(\text{pz})_2]_2\text{C}_6\text{H}_4$ (0.079 g, 0.21 mmol) was added by cannula to a 10-mL acetone solution of $[\text{Cd}_2(\text{thf})_5](\text{BF}_4)_4$ (0.10 g, 0.11 mmol). A white precipitate formed within 30 min of stirring at room temperature, and after a total of 16 h of stirring, the precipitate was isolated by filtration, washed with 5 mL of acetone, and dried in vacuo, yielding 0.10 g (79%) of a white solid. Single crystals suitable for X-ray studies were grown by the vapor diffusion of Et_2O into 1-mL CH_3CN solutions of **3** and taken directly from the mother liquor. Crystals for elemental analysis were removed from the mother liquor, rinsed with ether, and dried in vacuo. mp 213–214 °C. Anal. Calcd for $\text{C}_{40}\text{H}_{36}\text{B}_2\text{Cd}_2\text{F}_{10}\text{N}_{16}$: C, 40.81; H, 3.08; N, 19.04. Found: C, 40.43; H, 3.23; N, 18.80. IR (KBr, cm^{-1}): 3134, 1458, 1409, 1295, 1152, 1111, 1062, 764, 520. ¹H NMR (500 MHz, CD_3CN): δ 7.91 (s, 4 H, 3/5-pz), 7.85 (s, 2 H, $\text{CH}(\text{pz})_2$), 7.62 (s, 4 H, 3/5-pz), 7.40 (unresolved t, 1 H, 5- C_6H_4), 6.79 (br s, 2 H, 4,6- C_6H_4), 6.47 (s, 4 H, 4-pz), 5.94 (br s, 1 H, 2- C_6H_4). ¹³C NMR (126 MHz, CD_3CN): δ 143.8, 138.0, 135.2, 130.6, 128.4, 108.0, 75.9. ¹⁹F NMR (376 MHz, CD_3CN): δ −152. MS ESI(+) m/z (rel. % abund.) [assign]: 941 (1) $[\text{Cd}(\text{L}_m)_2(\text{BF}_4)]^+$, 571 (5) $[\text{Cd}(\text{L}_m)\text{BF}_4]^+$, 503 (1) $[\text{Cd}(\text{L}_m)\text{F}]^+$, 427 (20) $[\text{Cd}(\text{L}_m)_2]^{2+}$, 371 (80) $[\text{L}_m + \text{H}]^+$, 303 (100) $[\text{L}_m - \text{pz}]^+$.

$[\text{Zn}_2(\mu\text{-F})(\mu\text{-}1,3,5\text{-}[\text{CH}(\text{pz})_2]_3\text{C}_6\text{H}_3)_2](\text{BF}_4)_3$ (4). A solution of 1,3,5- $[\text{CH}(\text{pz})_2]_3\text{C}_6\text{H}_3$ (0.16 g, 0.31 mmol) in 10 mL of CH_2Cl_2 and 50 mL of acetone was added at once to a 10-mL acetone solution of $\text{Zn}(\text{BF}_4)_2 \cdot 5\text{H}_2\text{O}$ (0.10 g, 0.31 mmol). The resulting solution was stirred at room temperature for 2 days, during which time a fine white precipitate formed. Removal of the solvent, washing with 5 mL of acetone, and drying in vacuo left 0.14 g (64%) of **4** as a white solid. Crystals suitable for X-ray studies were grown by the vapor diffusion of Et_2O into 1-mL CH_3CN solutions of **4** and taken directly from the mother liquor. The

(15) Reger, D. L.; Collins, J. E. *Inorg. Synth.* **2004**, *34*, 91.

(16) (a) Sur, S. K. *J. Magn. Reson.* **1989**, *82*, 169. (b) Evans, D. F. *J. Chem. Soc.* **1959**, 2003.

Table 1. Crystal Data and Refinement Details for [Fe₂(μ-F)(μ-m-[CH(pz)₂]₂C₆H₄)₂](BF₄)₃·1.5CH₃CN (**1**·**1.5CH₃CN**), [Zn₂(μ-F)(μ-m-[CH(pz)₂]₂C₆H₄)₂](BF₄)₃·1.5CH₃CN (**2**·**1.5CH₃CN**), [Cd₂(μ-F)₂(μ-m-[CH(pz)₂]₂C₆H₄)₂](BF₄)₂ (**3**), and [Zn₂(μ-F)(μ-1,3,5-[CH(pz)₂]₃C₆H₃)₂](BF₄)₃ (**4**)

	1 · 1.5CH₃CN	2 · 1.5CH₃CN	3	4
empirical formula	C ₄₃ H _{40.50} B ₃ F ₁₃ Fe ₂ N _{17.50}	C ₄₃ H _{40.50} B ₃ F ₁₃ N _{17.50} Zn ₂	C ₄₀ H ₃₆ B ₂ Cd ₂ F ₁₀ N ₁₆	C ₅₄ H ₄₈ B ₃ F ₁₃ N ₂₄ Zn ₂
fw	1193.56	1212.60	1177.27	1443.33
<i>T</i> (K)	100(2)	150(1)	150(1)	150(1)
cryst syst	monoclinic	monoclinic	monoclinic	triclinic
space group	<i>P</i> 2 ₁ / <i>m</i>	<i>P</i> 2 ₁ / <i>m</i>	<i>P</i> 2 ₁ / <i>c</i>	<i>P</i> 1̄
<i>a</i> , Å	10.1402(6)	10.6471(5)	9.1312(5)	12.2690(4)
<i>b</i> , Å	42.645(3)	42.2320(18)	14.9574(8)	12.4716(4)
<i>c</i> , Å	11.7779(7)	11.3926(5)	16.3233(9)	22.2645(7)
α, deg	90	90	90	79.5610(10)
β, deg	101.8740(10)	101.1710(10)	100.4350(10)	87.1720(10)
γ, deg	90	90	90	70.0740(10)
<i>V</i> , Å ³	4984.1(5)	5025.6(4)	2192.5(2)	3149.53(17)
<i>Z</i>	4	4	2	2
<i>d</i> _{calcd} , Mg·m ⁻³	1.591	1.603	1.783	1.522
abs coeff, mm ⁻¹	0.685	1.056	1.066	0.859
cryst size, mm ³	0.32 × 0.20 × 0.10	0.38 × 0.22 × 0.16	0.18 × 0.06 × 0.04	0.22 × 0.16 × 0.10
final <i>R</i> indices [<i>I</i> > 2σ(<i>I</i>)]				
<i>R</i> 1	0.0574	0.0391	0.0408	0.0476
w <i>R</i> 2	0.1201	0.0963	0.0843	0.1044

unidentified solvent of crystallization found in the crystal structure could not be completely removed by drying. mp > 330 °C. IR (KBr, cm⁻¹): 3134, 1413, 1070, 915, 768, 706, 637. ¹H NMR (400 MHz, CD₃CN): δ 8.24 (d, *J* = 2.4 Hz, 4 H, 5/3-pz[Zn]), 8.19 (d, *J* = 2.4 Hz, 4 H, 5/3-pz[Zn]), 8.03 (s, 4 H, CH(pz)₂[Zn]), 7.87 (d, *J* = 1.6 Hz, 4 H, 5/3-pz[Zn]), 7.79 (s, 2 H, CH(pz)₂), 7.67 (br s, 4 H, 5/3-pz), 7.51 (br s, 4 H, 5/3-pz), 6.62 (t, *J* = 2.2 Hz, 4 H, 4-pz[Zn]), 6.56 (d, *J* = 1.6 Hz, 4 H, 5/3-pz[Zn]), 6.31 (t, *J* = 2.0 Hz, 4 H, 4-pz[Zn]), 6.28 (t, *J* = 2.4 Hz, 4 H, 4-pz), 5.99 (br s, 4 H, C₆H₃), 4.54 (s, 2 H, C₆H₃). ¹⁹F NMR (376 MHz, CD₃CN): δ -152 (BF₄⁻), -211 (Zn-F-Zn). MS ESI(+) *m/z* (rel. % abund.) [assign]: 1183 (5) [Zn(L³)₂BF₄]⁺, 1115 (1) [Zn(L³)₂F]⁺, 599 (1) [Zn(L³)F]⁺, 538 (30) [Zn(L³)₂]²⁺, 517 (100) [L³ + H]⁺.

Crystal Structure Determinations. X-ray intensity data from a colorless needle of **1**·**1.5CH₃CN**, colorless bars of **2**·**1.5CH₃CN** and **3**, and a colorless prism of **4** were measured at 100(2) K for **1**·**1.5CH₃CN** and 150(1) K for **2**·**1.5CH₃CN**, **3**, and **4** on a Bruker SMART APEX CCD-based diffractometer (Mo Kα radiation, λ = 0.71073 Å).¹⁷ Raw data frame integration and Lp corrections were performed with SAINT+.¹⁷ Final unit cell parameters were determined by least-squares refinement of 1569, 6744, 2701, and 6692 reflections from the data sets of **1**·**1.5CH₃CN**, **2**·**1.5CH₃CN**, **3**, and **4**, respectively. Analysis of the data showed negligible crystal decay during data collection. For compound **1**·**1.5CH₃CN**, an empirical absorption correction was applied with SADABS.¹⁷ Direct methods structure solution, difference Fourier calculations, and full-matrix least-squares refinement against *F*² were performed with SHELXTL.¹⁸ All non-hydrogen atoms were refined with anisotropic displacement parameters except where noted. Hydrogen atoms were placed in geometrically idealized positions and included as riding atoms. Details of the data collections are given in Table 1, while further notes regarding the solution and refinement for all four structures follow.

Systematic absences in the intensity data for **1**·**1.5CH₃CN** were consistent with the space groups *P*2₁/*m* and *P*2₁, the former of which was eventually confirmed by successful solution and refinement of the data. The asymmetric unit contains half each of two independent Fe cations, three BF₄⁻ anions, and two CH₃CN

molecules of crystallization. The cation associated with Fe(1) is situated about a crystallographic inversion center, and the Fe(2) cation is bisected by a mirror plane. The bridging F atoms of each cation are located on the respective symmetry elements. Two of the three BF₄⁻ anions display significant disorder. B(2) is disordered equally over two orientations about the B(2)–F(21) axis. A disorder model incorporating three orientations was employed for B(3). The occupancies for each B(3) disorder component were adjusted to give reasonable displacement parameters and then fixed. The final values are 0.4/0.4/0.2. Only the B and common apical F atoms were refined anisotropically for this species; all others were isotropic. A total of 150 restraints (SHELX SAME) were used in keeping the geometry of the disordered BF₄⁻ anions similar to that of the well-behaved anion B(1).

The compound **2**·**1.5CH₃CN** crystallizes in the space group *P*2₁/*m*, as indicated by the pattern of systematic absences in the intensity data and confirmed by the successful solution and refinement of the structure. The asymmetric unit consists of half each of two [Zn₂(μ-F)(μ-m-[CH(pz)₂]₂C₆H₄)₂]³⁺ cations, three independent BF₄⁻ counterions, and two acetonitrile molecules of crystallization. The cation associated with Zn(1) is situated about a crystallographic inversion center, and the Zn(2) cation is bisected by a mirror plane. One BF₄⁻ ion (B3) is disordered and was modeled with two equally populated orientations. The geometries of both disorder components were restrained to be similar to that of an ordered BF₄⁻ (B1) with SHELX SAME instructions (30 restraints). Some elongated fluorine atom displacement ellipsoids indicate more than two orientations are actually present throughout the crystal.

Compound **3** crystallizes in the space group *P*2₁/*c*, as determined uniquely by the pattern of systematic absences in the intensity data. The asymmetric unit consists of half of a [Cd₂(μ-F)₂(μ-m-[CH(pz)₂]₂C₆H₄)₂]²⁺ cation located on an inversion center and one BF₄⁻ anion.

Compound **4** crystallizes in the triclinic system. The space group *P*1̄ was confirmed by the successful solution and refinement of the data. The asymmetric unit consists of half each of two independent [Zn₂(μ-F)(μ-1,3,5-[CH(pz)₂]₃C₆H₃)₂]³⁺ complexes, three BF₄⁻ anions, and a small region of unidentified solvent. Both independent [Zn₂(μ-F)(μ-1,3,5-[CH(pz)₂]₃C₆H₃)₂]³⁺ cations reside on crystallographic inversion centers. Atoms of these complexes were numbered identically except for the suffix "A" or "B". One of the BF₄⁻ anions (B3) is disordered and was modeled as occupying three

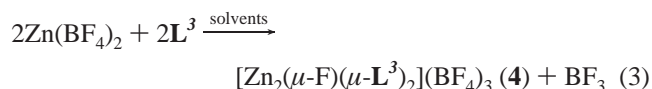
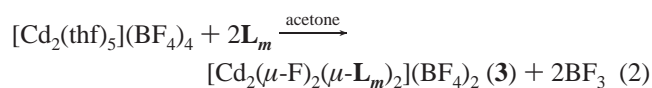
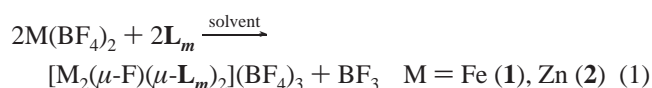
(17) SMART Version 5.625, SAINT+ Version 6.22 and SADABS Version 2.05; Bruker Analytical X-ray Systems, Inc.: Madison, WI, 2001.

(18) Sheldrick, G. M. SHELXTL Version 6.14; Bruker Analytical X-ray Systems, Inc.: Madison, WI, 2000.

distinct orientations. Occupancies for each orientation were refined, subject to the constraint that they sum to unity. A total of 61 distance restraints were employed to maintain a chemically reasonable geometry for each component. These atoms were refined isotropically. Despite the small volume occupied by the disordered solvent molecules (191.1 Å³ per unit cell, 6.1% of the total unit cell volume), no reasonable model could be achieved for these species, and their contribution to the structure factors was removed with SQUEEZE (48 e⁻/cell).¹⁹ From trial modeling attempts, these species may be a mixture of acetonitrile and water. The reported FW, d_{calcd} and $F(000)$ reflect known unit cell contents only.

Results

Syntheses. Compounds **1** and **2** were prepared by combining separate THF or acetone solutions of \mathbf{L}_m and $\text{Fe}(\text{BF}_4)_2 \cdot 6\text{H}_2\text{O}$ or $\text{Zn}(\text{BF}_4)_2 \cdot 5\text{H}_2\text{O}$, according to eq 1. In the same way, **3** was formed upon the mixing of acetone solutions of $[\text{Cd}_2(\text{thf})_5](\text{BF}_4)_4$ and \mathbf{L}_m , as given in eq 2. The complexes precipitated from solution as fine white powders. Elemental analyses performed on vacuum-dried crystals of **1–3** were consistent with the solvent-free formulas given in the equations, and X-ray crystallographic studies, discussed below, confirmed the fluoride-bridged, metallacyclic structures.



Complex **4** was prepared by adding an acetone/ CH_2Cl_2 solution of \mathbf{L}^3 to an acetone solution of $\text{Zn}(\text{BF}_4)_2 \cdot 5\text{H}_2\text{O}$ (eq 3). The product precipitated from solution after 2 days. X-ray crystallographic studies confirmed the metallacyclic solid-state structure, similar to the structures of **1–3**, and also containing an unbound bis(pyrazolyl)methane ligating site for each ligand in the metallacycle. In an attempt to coordinate a different metal to this unbound site, the addition of excess AgBF_4 to a solution of **4** yielded crystals, but X-ray analysis showed these crystals to be highly disordered and the structure could not be completely solved. These crystals could be shown, however, to contain metallacycles linked through coordination of silver(I) cations by the third bis-(pyrazolyl)methane unit, but because it appears that the silver cations randomly replaced some of the zinc cations in the metallacycles, no further characterization of this product could be obtained.

Despite the presence of water molecules in the hydrated iron and zinc starting materials, the major products are the fluoride-bridged species, and no water-coordinated complexes are isolated. Furthermore, the possibility that hydroly-

sis of BF_4^- , rather than abstraction, is the source of fluoride has been ruled out by the detection of a BF_3 -solvent adduct in ¹⁹F NMR spectra of the crude products, as well as the lack of detection of BF_4^- hydrolysis products in any of these systems. Abstraction and not hydrolysis must be the pathway in the cadmium system where all reagents are rigorously anhydrous.

The silaphilicity of the bridging fluoride ligands in the zinc and cadmium complexes **2** and **3** was investigated by treating the complexes with bis(trimethylsilyl)acetylene ($\text{Me}_3\text{SiCCSiMe}_3$) and triethylsilane (Et_3SH).^{5,20} No reaction took place between the zinc complex and either silane reagent; only starting materials were recovered. The reactions between the cadmium complex and the silane reagents resulted in decomposition of the starting material.

NMR. The proton NMR spectrum of the iron complex **1** displays the broadened signals and expanded chemical shift range expected of a paramagnetic compound, and the observed resonances cannot be assigned with confidence. No signals are observed in the ¹³C NMR spectrum of **1**, and only BF_4^- is observed in its ¹⁹F NMR spectrum. By analogy to the zinc complexes described below, the fluoride-bridged dimers of **1** are assumed to be intact in acetonitrile. The solution magnetic moment of **1**, determined by the Evans method,¹⁶ is 6.2 μ_B per dimer. This value is identical to the moment observed for the di-fluoride-bridged iron(II) dimer prepared recently by Holland and co-workers.⁵

NMR spectra of the analogous, diamagnetic zinc complex **2** indicate the fluoride-bridged dimeric structure remains intact in acetonitrile. In the ¹H spectrum, only three resonances are observed for the two *m*-phenylene spacers, indicating the two rings are equivalent, as are the four $-\text{CH}(\text{pz})_2$ methine hydrogen atoms, which resonate at 8.11 ppm. In contrast, two distinct equal-intensity environments for the pyrazolyl protons are observed. One set of 3/5-pyrazolyl protons resonates at 8.39 and 8.16 ppm, and the other set resonates at 7.38 and 6.63 ppm. The 4-pyrazolyl protons resonate at 6.50 and 6.40 ppm for the two sets. Consideration of the solid-state structures where one of the two nonequivalent dimers has a center of symmetry and the other mirror symmetry (see bottom of Figure 4) leads to the conclusion that the intact solution structure would have two types of pyrazolyl rings, those along the Zn–F–Zn axis and those perpendicular to it, and that the *m*-phenylene spacers and $-\text{CH}(\text{pz})_2$ methine hydrogen atoms should be equivalent, respectively, as observed. Importantly, the bridging fluoride ligand gives rise to a signal in the ¹⁹F NMR spectrum at -211 ppm, and the signal from BF_4^- is found downfield at -150 ppm. The ¹H NMR signals in **2** do not show any line-broadening up to 75 °C, indicating thermal stability of the complexes. The ¹³C NMR spectrum of **2** is consistent with the deduced fluoride-bridged dimeric structure, showing two sets of pyrazolyl resonances (the two 4-pyrazolyl signals are

(19) Spek, A. L. *PLATON, A Multipurpose Crystallographic Tool*; Utrecht University: Utrecht, The Netherlands, 1998.

(20) (a) Hao, H.; Cui C.; Roeky, H. W.; Bai, G.; Schmidt, H.-G.; Noltemeyer, M. *Chem. Commun.* **2001**, 1118. (b) Hoffman, N. W.; Prokopuk, N.; Robbins, M. J.; Jones, C. M.; Doherty, N. M. *Inorg. Chem.* **1991**, *30*, 4177. (c) Doherty, N. M.; Critchlow, S. C. *J. Am. Chem. Soc.* **1987**, *109*, 7906.

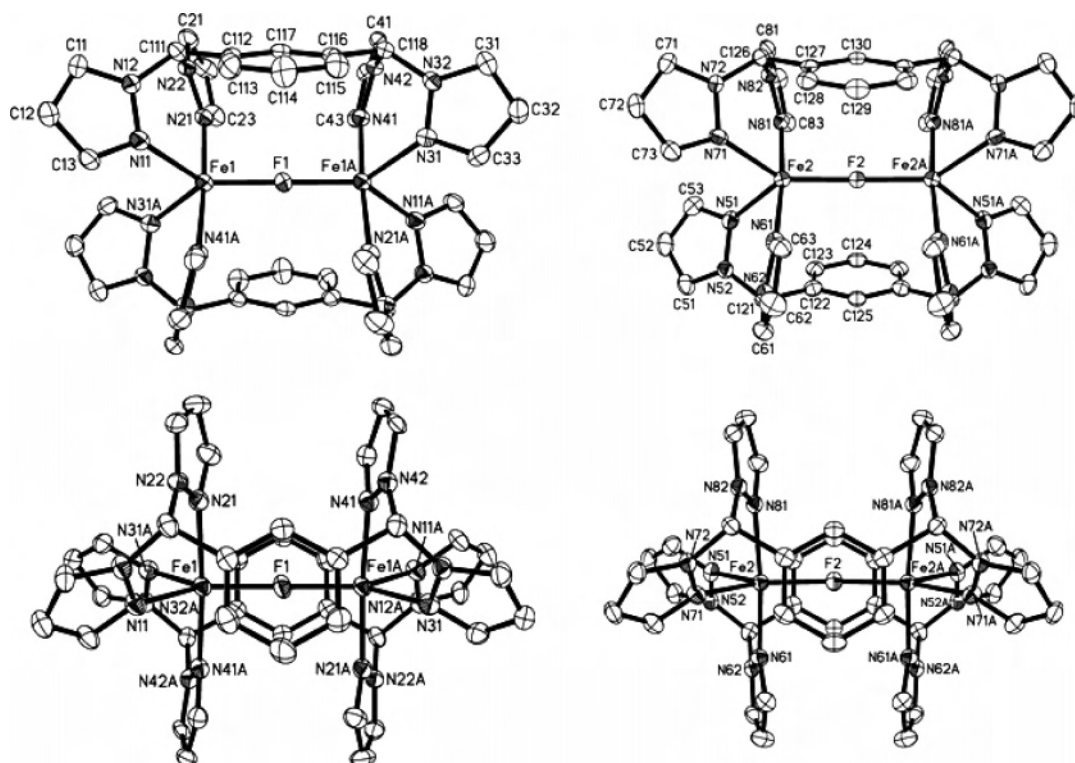


Figure 4. Orthogonal views of the independent cations of $[\text{Fe}_2(\mu\text{-F})(\mu\text{-}m\text{-}[\text{CH}(\text{pz})_2]_2\text{C}_6\text{H}_4)_2](\text{BF}_4)_3 \cdot 1.5\text{CH}_3\text{CN}$ (**1**·**1.5CH₃CN**) located on an inversion center (left) and a mirror plane (right). Hydrogen atoms are omitted for clarity. Displacement ellipsoids are drawn at the 50% probability level. Analogous cations are present in $[\text{Zn}_2(\mu\text{-F})(\mu\text{-}m\text{-}[\text{CH}(\text{pz})_2]_2\text{C}_6\text{H}_4)_2](\text{BF}_4)_3 \cdot 1.5\text{CH}_3\text{CN}$ (**2**·**1.5CH₃CN**). Selected bond distances (Å) and angles (deg) for **1**·**1.5CH₃CN**: Fe(1)–F(1) 1.9441(6), Fe(1)–N(11) 2.126(3), Fe(1)–N(21) 2.146(3), Fe(1)–N(31A) 2.130(3), Fe(1)–N(41A) 2.133(3), Fe(2)–F(2) 1.9752(6), Fe(2)–N(51) 2.145(3), Fe(2)–N(61) 2.131(3), Fe(2)–N(71) 2.157(3), Fe(2)–N(81) 2.143(3); N(11)–Fe(1)–F(1) 134.12(10), N(11)–Fe(1)–N(31A) 93.70(13), N(31A)–Fe(1)–F(1) 132.18(9), N(11)–Fe(1)–N(21) 87.10(13), N(21)–Fe(1)–F(1) 91.50(9), N(21)–Fe(1)–N(41A) 175.90(13), Fe(1)–F(1)–Fe(1A) 180.00(3). Selected bond distances (Å) and angles (deg) for **2**·**1.5CH₃CN**: Zn(1)–F(1) 1.9385(3), Zn(1)–N(11) 2.073(2), Zn(1)–N(21) 2.123(2), Zn(1)–N(31A) 2.081(2), Zn(1)–N(41A) 2.117(2), Zn(2)–F(2) 2.0056(4), Zn(2)–N(51) 2.125(2), Zn(2)–N(61) 2.113(2), Zn(2)–N(71) 2.096(2), Zn(2)–N(81) 2.106(2); N(11)–Zn(1)–F(1) 130.43(6), N(11)–Zn(1)–N(31A) 99.05(9), N(31A)–Zn(1)–F(1) 130.52(6), N(11)–Zn(1)–N(21) 88.50(9), N(21)–Zn(1)–F(1) 89.29(6), N(21)–Zn(1)–N(41A) 179.70(9), Zn(1)–F(1)–Zn(1A) 179.996(1).

unresolved), as well as one signal from the four equivalent methine carbon atoms and one set of signals from the two equivalent phenylene rings.

Analysis of the cadmium complex **3** in acetonitrile solution is complicated by severe line broadening in the ^1H NMR spectra and, to a lesser extent, in the ^{13}C NMR spectra. The measured proton T_2 relaxation times for **3** in CD_3CN (10–70 ms) are at least an order of magnitude shorter than expected for this complex and explain the observed line broadening. The observation of only one set of ligand signals in CD_3CN indicates an average structure in which the macrocyclic structure is not retained or some complex intra- or intermolecular dynamic process is taking place. The lack of change in the proton spectrum in the temperature range of -35 to 75 °C, however, suggests exchange processes are unlikely to be the cause of the line-broadening, although they cannot be completely ruled out. The ^{13}C NMR data are consistent with this conclusion, showing only one set of ligand signals, and only the expected BF_4^- signal is clearly observed in the ^{19}F NMR spectrum. No resonances are observed in the ^{113}Cd NMR spectrum of **3**, likely a consequence of signal broadening as observed in the ^1H and ^{13}C NMR spectra.

The ^1H NMR spectrum of **4** shows that the metallacycles in **4** are intact in solution, as observed for compound **2**. Thus,

two sets of coordinated bis(pyrazolyl)methane signals are observed, and they correspond to the units bound to the zinc cations in the fluoride-bridged dimer: 8.24 and 8.19 ppm for the 3/5-pyrazolyl protons in one set and 7.87 and 6.56 ppm for the other set; 6.62 and 6.31 ppm for the 4-pyrazolyl protons. The four equivalent methine protons resonate at 8.03 ppm. The aromatic protons attached to the central arene linker reside in two distinct environments. Two protons are adjacent to both a coordinated and uncoordinated bis-(pyrazolyl)methane site, and they resonate together at 5.99 ppm. The third proton is adjacent to two coordinated sites and is shielded compared to the others, resonating at 4.54 ppm. The uncoordinated bis(pyrazolyl)methane sites are also equivalent and show slightly broadened signals, with chemical shifts that closely match those of the free ligand, **L³** (3/5-pyrazolyl protons: 7.67 and 7.51 ppm in **4** vs 7.56 and 7.49 ppm in **L³**; 4-pyrazolyl protons: 6.28 in **4** vs 6.27 ppm in **L³**; methine protons: 7.79 in **4** vs 7.72 ppm in **L³**). Also similar to **2**, the ^{19}F NMR spectrum of **4** shows a highly shielded signal at -211 ppm, due to the bridging fluoride ligand, in addition to the BF_4^- signal at -152 ppm.

Mass Spectrometry. Positive-ion electrospray mass spectra of all four complexes are similar. No clusters are observed that correspond to the complete fluoride-bridged dimeric cations, $[\text{M}_2\text{L}_2\text{F}]^{3+}$ ($\text{M} = \text{Fe}, \text{Zn}; \text{L} = \text{L}_m, \text{L}^3$) or $[\text{Cd}_2\text{-}$

$(L_m)_2F_2]^{2+}$, or any analogous cations associated with BF_4^- counterions. Fragments of these metallacycles, however, are consistently detected, albeit in low abundance. Each spectrum exhibits clusters of peaks for the species $[ML_2BF_4]^+$, $[MLF]^+$, and $[ML_2]^{2+}$. All but the spectrum of the cadmium complex contain the $[ML_2F]^+$ fragment. The mass spectrum of the cadmium complex, however, does uniquely show the species $[MLBF_4]^+$. The base peak in the spectrum of each complex is ligand-based, either $[HL]^+$ or $[L - pz]^+$.

Solid-State Structures. ORTEP drawings of the two independent, fluoride-bridged dimeric cations in $1 \cdot 1.5CH_3CN$ are shown in Figure 4. The zinc complex $2 \cdot 1.5CH_3CN$ is isostructural and isomorphous with $1 \cdot 1.5CH_3CN$. The structures of $1 \cdot 1.5CH_3CN$ and $2 \cdot 1.5CH_3CN$ are unusual in that one of the two independent complex ions (associated with Fe(1) and Zn(1)) resides on an inversion center whereas the other (associated with Fe(2) and Zn(2)) rests on a plane of symmetry. The coordination geometries about the metal cations are trigonal bipyramids that share a common vertex at the bridging fluoride ligand. The Fe(1) and Zn(1) are equatorially bound through the coplanar atoms N(11), N(31A), and F(1) and axially bound through N(21) and N(41A). Although the angles between atoms in the equatorial planes are somewhat distorted (e.g., 94° , 132° , and 134°), the angles between the axial atoms and those in the equatorial planes are at near right angles to each other (e.g., 87° and 89°).

In both $1 \cdot 1.5CH_3CN$ and $2 \cdot 1.5CH_3CN$, the metal–fluoride bonds of the second cation, which has mirror symmetry, are longer than those of the first, centrosymmetric cation (1.944 vs 1.975 Å for $1 \cdot 1.5CH_3CN$; 1.938 vs 2.006 Å for $2 \cdot 1.5CH_3CN$). This difference in metal–fluoride bond distance is greater in the zinc complex. Interestingly, the Fe–F bond distance in the first cation (1.944 Å) is slightly longer than the respective Zn–F distance (1.938 Å), but the second Fe–F bond distance (1.975 Å) is shorter than the respective Zn–F distance (2.006 Å). This feature is in contrast to the Zn–N distances in $2 \cdot 1.5CH_3CN$, which are shorter than the respective Fe–N distances in $1 \cdot 1.5CH_3CN$ by a little over 0.03 Å, on average, the difference in the ionic radii of the two metals, and are very close to what would be predicted from the sum of the radii.²¹ In contrast, the metal–fluoride distances average to about the same values of 1.96 Å for iron and 1.97 Å for zinc, which make the iron values shorter than would be predicted (2.0 Å).

An ORTEP drawing of the dimeric cation of the cadmium complex **3** is shown in Figure 5. The complex contains two bridging fluoride ligands, rather than the one observed for the zinc and iron complexes described above. The Cd–F distances are similar but not identical (2.19 and 2.23 Å). Each cadmium ion resides in a distorted octahedral environment. The angles between atoms at opposite apices of the octahedra, for instance, are all significantly less than 180° (166° , 156° , and 168°). The distance between the cadmium ions, 3.31 Å, is shorter than the metal···metal distances in the previous two complexes. Despite the larger ionic radius of

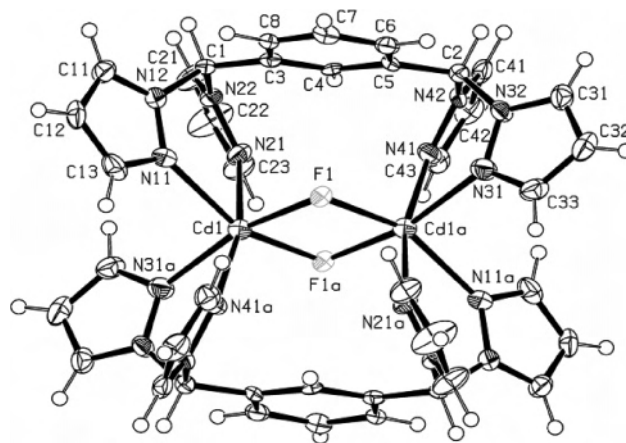


Figure 5. ORTEP representation of the cationic dimer in $[Cd_2(\mu-F)_2(\mu-m-[CH(pz)_2]_2C_6H_4)_2](BF_4)_2$ (**3**). Displacement ellipsoids are drawn at the 50% probability level. Selected bond distances (Å) and angles(deg): Cd(1)–F(1) 2.191(3), Cd(1)–F(1a) 2.229(3), Cd(1)–N(11) 2.357(4), Cd(1)–N(21) 2.359(4), Cd(1)–N(31a) 2.342(4), Cd(1)–N(41a) 2.377(4); F(1)–Cd(1)–N(11) 92.41(13), F(1)–Cd(1)–F(1a) 82.95(11), Cd(1)–F(1)–Cd(1a) 97.05(10), F(1)–Cd(1)–N(31a) 165.88(14), N(11)–Cd(1)–N(21) 79.21(15), N(11)–Cd(1)–F(1a) 155.69(13), N(11)–Cd(1)–N(41a) 92.99(15), N(11)–Cd(1)–N(31a) 96.42(16), N(21)–Cd(1)–N(41a) 167.53(15).

Cd^{2+} , bent rather than linear Cd–F–Cd angles (97° vs 180°) in **3** result in a significant decrease in Cd···Cd distance.

The crystalline structure of **4** is similar to the structures of $1 \cdot 1.5CH_3CN$ and $2 \cdot 1.5CH_3CN$ in that it also contains two crystallographically independent complex ions, types A and B, with type A shown in Figure 6. Unique to **4** is that both ions, rather than just one, reside on inversion centers. Like the iron and zinc analogues of the bitopic ligand described above, a single fluoride ligand in **4** serves as the common vertex shared by the two trigonal bipyramidally coordinated zinc cations. The three atoms equatorially coordinated to Zn(1A) (F(1A), N(21A), and N(31A)) are coplanar and separated by angles of 103° , 127° , and 130° . The axial atoms (N(11A) and N(41A)) are nearly 90° from each of the equatorial atoms and make a Zn(1A)-centered angle of 180° with each other. The coordination environment around Zn(1B) has similar dimensions (see Figure 6). The Zn–F bond distances in **4** are 1.95 and 1.93 Å for Types A and B, respectively. They are just slightly shorter than the Fe–F and Zn–F distances in $1 \cdot 1.5CH_3CN$ and $2 \cdot 1.5CH_3CN$. The most salient difference between **4** and the complexes $1 \cdot 1.5CH_3CN$ and $2 \cdot 1.5CH_3CN$ above is the presence in **4** of an uncoordinated bis(pyrazolyl)methane site on each of the two ligands in the complex. The supramolecular structure of **4**, as well as the structures of $1 \cdot 1.5CH_3CN$, $2 \cdot 1.5CH_3CN$, and **3**, is organized by a variety of noncovalent interactions such as π – π , CH– π , and CH–F interactions, and these features for each complex are discussed in the Supporting Information.

Discussion

Fluoride Abstraction. We have shown that alkylidene- and *m*-arene-linked bis(pyrazolyl)methane ligands consistently direct formation of dimeric silver metallacycles, rather than the formation of coordination polymers, in the presence of weakly coordinating counterions, such as BF_4^- , without

(21) Shannon, R. D. *Acta Crystallogr.* **1976**, A32, 751.

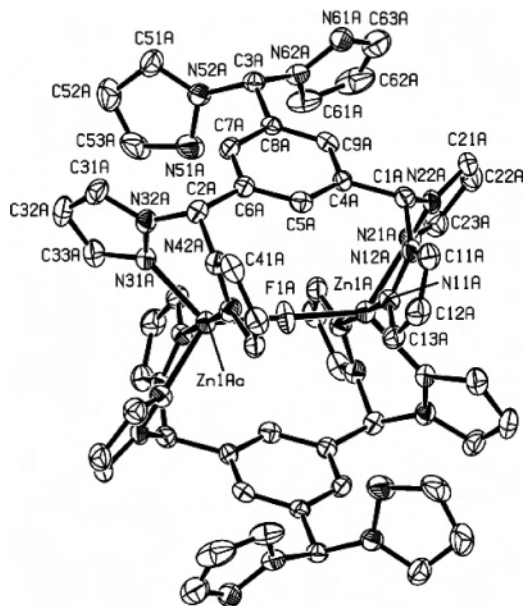


Figure 6. ORTEP drawing of one of the two independent cations present in the crystal structure of $[\text{Zn}_2(\mu\text{-F})(\mu\text{-}1,3,5\text{-}[\text{CH}(\text{pz})_2]_3\text{C}_6\text{H}_3)_2](\text{BF}_4)_3$ (**4**). The second independent cation is assigned the same numbering scheme using the designation "B". Hydrogen atoms are omitted for clarity. Displacement ellipsoids are drawn at the 50% probability level. Selected bond distances (Å) and angles (deg): Zn(1A)–F(1A) 1.9496(4), Zn(1A)–N(11A) 2.095(3), Zn(1A)–N(21A) 2.084(3), Zn(1Aa)–N(31A) 2.073(3), Zn(1Aa)–N(41A) 2.123(3), Zn(1B)–F(1B) 1.9300(4), Zn(1B)–N(11B) 2.136(3), Zn(1B)–N(21B) 2.094(3), Zn(1Ba)–N(31B) 2.088(3), Zn(1Ba)–N(41B) 2.118(3); F(1A)–Zn(1A)–N(21A) 127.14(8), F(1A)–Zn(1Aa)–N(31A) 129.83(8), N(21A)–Zn(1A)–N(31Aa) 103.01(10), F(1A)–Zn(1A)–N(11A) 90.08(7), N(11A)–Zn(1A)–N(21A) 89.12(11), N(11A)–Zn(1A)–N(31Aa) 91.96(11), N(11A)–Zn(1A)–N(41Aa) 179.62(11), Zn(1A)–F(1A)–Zn(1Aa) 180.0, F(1B)–Zn(1B)–N(21B) 132.24(8), F(1B)–Zn(1B)–N(31Ba) 128.66(8), N(21B)–Zn(1B)–N(31Ba) 99.07(11), F(1B)–Zn(1B)–N(11B) 93.86(8), N(11B)–Zn(1B)–N(21B) 86.96(11), N(11B)–Zn(1B)–N(31Ba) 89.95(12), N(11B)–Zn(1B)–N(41Ba) 177.63(11), Zn(1B)–F(1B)–Zn(1Ba) 180.0.

concomitant fluoride abstraction.^{12a,b,22} In the current work with divalent iron, zinc, and cadmium, we again observe metallacycles, but in these systems, coordination by the fluoride ion abstracted from BF_4^- stabilizes the coordination environments of the divalent cations within the metallacycles. Whereas four-coordination (or even three) is favorable for the Ag^+ cation, five- or six-coordination is apparently required for the cationic metallacycles in the present study. Divalent iron and zinc are sufficiently hard cations to effect abstraction of the hard fluoride anion, thereby increasing the coordination number of the metal.

In iron complexes containing bridging fluoride, the cations most commonly reside in octahedral environments. Of the complexes that contain a single fluoride ligand bridging two iron centers, most have bent Fe–F–Fe angles (between 90° and 170°),²³ but a few are nearly linear (177° is the closest).²⁴ Compound **1** reported here, therefore, represents a rare example of a structurally characterized, discrete iron(II) compound with a linear fluoride bridge and, to our knowledge, the first discrete fluoride-bridged complex containing five-coordinate iron(II) cations. Holland has recently reported the first crystal structures of discrete iron(II) fluoride complexes, including a di-fluoride-bridged dimer with four-coordinate Fe^{2+} and a terminal fluoride complex with

three-coordinate Fe^{2+} .⁵ The bridging Fe–F bonds average 1.98 Å in length, very similar to the Fe–F bond distances (1.94 and 1.98 Å) in **1**. For comparison, the terminal Fe–F bond in Holland's compound measures 1.81 Å.

Few discrete fluoride-bridged zinc complexes have been structurally characterized by crystallographic means.²⁵ An unambiguous linear fluoride bridge between two zinc cations was recently prepared using a ligand that resembles L_m , comprising bis(imidazolyl)methylene groups linked by a pyridine ring in a meta fashion.²⁶ That compound and the compounds **2** and **4** reported here are the only examples of linear Zn–F–Zn linkages in discrete coordination complexes. Numerous examples of fluoride ions bridging zinc cations in extended networks are known, and their Zn–F distances usually fall within the range of 1.95–2.10 Å.^{25–27} Terminal fluoride ligands on zinc are less common, and their Zn–F distances are typically shorter (ca. 1.85 Å),²⁸ although a long terminal Zn–F bond of 2.04 Å has been claimed.²⁹ The complexes **2** and **4**, therefore, contain typical bridging Zn–F bond distances (1.94 and 2.01 Å for **2**; 1.93 and 1.95 Å for **4**).

The larger and softer Cd^{2+} ion has a lower affinity for fluoride, but its strong preference for six-coordination drives the fluoride abstraction to form the difluoride-bridged **3**. Compound **3** is the first example of a crystallographically characterized, discrete fluoride-bridged cadmium complex. Extended networks containing Cd–F bonds where the fluoride ions act as bridging ligands have been reported, with typical Cd–F bond distances in the range of 2.26–2.29 Å.³⁰ The bridging Cd–F distances reported in this work (2.19, 2.23 Å) are comparatively short.

- (22) Reger, D. L.; Watson, R. P.; Smith, M. D. *Inorg. Chem.* **2006**, *45*, 10077–10087.
- (23) For example: (a) Choudhury, A.; Natarajan, S. *J. Solid State Chem.* **2000**, *154*, 507. (b) Cavellac, M.; Riou, D.; Ferey, G. *J. Solid State Chem.* **1994**, *112*, 441. (c) Dan, M. *J. Mol. Struct.* **2004**, *706*, 127. (d) Luo, S.-H.; Jiang, Y.-C.; Wang, S.-L.; Kao, H.-M.; Lii, K.-H. *Inorg. Chem.* **2001**, *40*, 5381. (e) Chakrabarti, S.; Natarajan, S. *Angew. Chem., Int. Ed.* **2002**, *41*, 1224. (f) Rao, C. N. R.; Sampathkumar, E. V.; Nagarajan, R.; Paul, G.; Behera, J. N.; Choudhury, A. *Chem. Mater.* **2004**, *16*, 1441. (g) Rao, C. N. R.; Paul, G.; Choudhury, A.; Sampathkumar, E. V.; Raychaudhuri, A. K.; Ramasesha, S.; Rudra, I. *Phys. Rev. B: Condens. Matter* **2003**, *67*, 134425. (h) Bino, A.; Ardon, M.; Lee, D.; Spingler, B.; Lippard, S. J. *J. Am. Chem. Soc.* **2002**, *124*, 4578. (i) Herold, S.; Lippard, S. J. *Inorg. Chem.* **1997**, *36*, 50.
- (24) (a) Leo, R.; Massa, W.; Pebler, J. *J. Fluorine Chem.* **2004**, *125*, 923. (b) Westerheide, L.; Müller, F. K.; Than, R.; Krebs, B.; Dietrich, J.; Schindler, S. *Inorg. Chem.* **2001**, *40*, 1951. (c) Choudhury, A.; Rao, C. N. R. *J. Struct. Chem.* **2002**, *43*, 632.
- (25) (a) Hao, H.; Cui, C.; Herbert, W. Bai, G.; Schmidt, H.-G.; Noltemeyer, M. *Chem. Commun.* **2001**, 1118. (b) Yu, P.; Müller, P.; Roesky, H. W.; Noltemeyer, M.; Demsar, A.; Uson, I. *Angew. Chem., Int. Ed.* **1999**, *38*, 3319. (c) Mrak, M.; Helliwell, M.; Ristic, A.; Logar, N. Z.; Kaucic, V. *Acta Chim. Slov.* **2001**, *48*, 147. (d) Wang, C.-M.; Liao, C.-H.; Kao, H.-M.; Lii, K.-H. *Inorg. Chem.* **2005**, *44*, 6294.
- (26) Worm, K.; Chu, F.; Matsumoto, K.; Best, M. D.; Lynch, V.; Anslyn, E. V. *Chem.–Eur. J.* **2003**, *9*, 741.
- (27) (a) Su, C. Y.; Goforth, A. M.; Smith, M. D.; Pellechia, P. J.; zur Loye, H.-C. *J. Am. Chem. Soc.* **2004**, *126*, 3576. (b) Larsen, F. K.; Overgaard, J.; Parsons, S.; Rentschler, E.; Smith, A. A.; Timco, G. A.; Wimpenny, R. E. P. *Angew. Chem., Int. Ed.* **2003**, *42*, 5978. (c) Maggard, P. A.; Stern, C. L.; Poeppelmeier, K. R. *J. Am. Chem. Soc.* **2001**, *123*, 7742.
- (28) (a) Weis, K.; Vahrenkamp, H. *Inorg. Chem.* **1997**, *36*, 5592. (b) Kläui, W.; Schilde, U.; Schmidt, M. *Inorg. Chem.* **1997**, *36*, 1598. (c) Tesmer, M.; Shu, M.; Vahrenkamp, H. *Inorg. Chem.* **2001**, *40*, 4022.
- (29) Hahn, F. E.; Jocher, C.; Lügger, T.; Pape, T. *Z. Anorg. Allg. Chem.* **2003**, *629*, 2341.

The presence of only one, rather than two, fluoride bridges in the iron and zinc compounds is a consequence of our use of the third-generation ligands L_m and L^3 with designed geometric preferences. Related compounds of first- and second-transition-series metals, including iron and cadmium, made by Reedijk using monotopic bis(3,5-dimethyl-1-pyrazolyl)methane ligands consisted of dibridged structures.⁸ Unique to our bis(pyrazolyl)methane systems is that the ligating sites are linked through a *m*-phenylene ring. Ligation of only one F^- ion apparently provides a sufficiently stable coordination environment for the iron and zinc compounds in the metallacycles formed by these linked ligands, and the desire for six-coordination is not strong enough to facilitate further BF_4^- activation. The arene linker of the bis-(pyrazolyl)methane ligands may provide some degree of steric deterrent for further F^- ligation, but the fact that the cadmium complex **3** is dibridged proves that two fluoride ligands may be included within the metallacyclic structure. The desire by cadmium for six-coordination overcomes any steric protection provided by the linked ligands.

In a more general sense, the ligands L_m and L^3 are best described as “fixed” but not necessarily “rigid” because, although the relative distances between bis(pyrazolyl)methane ligating sites (the central methine carbon atoms of the bis(pyrazolyl)methane units) remain essentially constant for all the complexes formed from these ligands, rotation of the bis(pyrazolyl)methane units about the methine–arene carbon (ipso) bond allows variation in the way the ligands bind metal centers. These ligands clearly favor the formation of the $[L_2M_2]^{n+}$ dimers with metal systems that lack other strongly bonded ligands, but the flexibility imparted by the rotation of the bis(pyrazolyl)methane units allows metal separations that stabilize silver complexes (average $Ag\cdots Ag$ separation of 4.64 Å) that show no fluoride abstraction;²² complexes with linear $M-F-M$ bonds that have average $M\cdots M$ separations of 3.92 Å; and a dibridged CdF_2Cd core where the $M\cdots M$ separation drops to 3.31 Å. These designed, fixed-geometry ligands, which readily support the $[L_2M_2]^{n+}$ dimeric metallacycles, are believed to promote fluoride abstraction by bringing two coordinatively unsaturated metals into a favorable position for bimetallic cooperativity (see Figure 1).

Solution Structures. The contrast in the behaviors of the zinc and cadmium complexes in acetonitrile provides another example of the sometimes dramatic differences in the chemistries of first- and second-transition-series congeners. The fluoride-bridged zinc dimers **2** and **4** remain intact in acetonitrile. 1H NMR spectra show two distinct environments for the coordinated pyrazolyl groups and a resonance for the bridging fluoride ligands at -211 ppm in ^{19}F NMR experiments. In contrast, the cadmium complex **3** affords spectra

containing severely broadened signals, where they can be observed, providing no indication of the difluoride-bridged cations that exist in the solid state. The signal broadening in the 1H NMR spectra of **3** is a result of short T_2 relaxation times that could arise from extensive aggregation in solution or from exchange processes, although the latter cause is less likely because there is no change in the line widths of the 1H NMR signals in **3** between -35 and 75 °C.

Previously reported transition and main group metal complexes containing bridging fluoride ligands exhibit a wide range of shielded resonances in their ^{19}F NMR spectra. For example, values of -141 , -228 , and -387 ppm, all referenced to $CFCl_3$, have been reported for iron,^{25b} molybdenum,⁶ and palladium³¹ complexes, respectively. Similarly, bridging fluoride ligands in aluminum (-121 to -168 ppm),³² silicon (-117 , -144),³³ and tin (-84)³⁴ compounds are also frequently highly shielded. The chemical shifts of the fluoride ligands in compounds **2** and **4** (-211 ppm) in the present work are in the range of these reported values. The variation in shielding of the fluoride ligands in these compounds is indicative of the relative donation of electron density from the electropositive metal centers to the electronegative fluoride, but direct correlations between the magnitude of this shielding and the nature of the metal–fluoride interactions are complicated by the large role that the paramagnetic shielding term plays in fluorine chemical shifts, in addition to the better understood diamagnetic shielding term.³⁵

The robustness of the fluoride-bridged zinc metallacycles is demonstrated by their inertness toward the silane reagents $Me_3SiCCSiMe_3$ and Et_3SiH , which may be explained by the reagents' inability to access the fluoride ligand held tightly within the metallacyclic core. The cadmium complex **3** is affected by these silane reagents, but decomposition appears to be the major reaction.

Summary

The *m*-arene-linked ligands L_{py} , L_m , and L^3 have been shown to promote formation of metallacyclic dimeric cations²² in analogous fashion to the more flexible, alkylidene-linked bis(pyrazolyl)methane ligands^{12a,b} reported earlier. For these arene-linked ligands, formation of metal-

(30) (a) Izumi, H. K.; Kirsch, J. E.; Stern, C. L.; Poeppelmeier, K. R. *Inorg. Chem.* **2005**, *44*, 884. (b) Halasyamani, P. S.; Heier, K. R.; Norquist, A. J.; Stern, C. L.; Poeppelmeier, K. R. *Inorg. Chem.* **1998**, *37*, 369. (c) Pickardt, J.; Kuhn, B. Z. *Naturforsch., B: Chem. Sci.* **1996**, *51*, 1701. (d) Maggard, P. A.; Kopf, A. L.; Stern, C. L.; Poeppelmeier, K. R.; Halasyamani, P. S. *Inorg. Chem.* **2002**, *41*, 4852. (e) Guillory, P. C. R.; Kirsch, J. E.; Izumi, H. K.; Stern, C. L.; Poeppelmeier, K. R. *Cryst. Growth Des.* **2006**, *6*, 382.

(31) Braun, T.; Steffen, A.; Schorlemer, V.; Neumann, B.; Stammler, H.-G. *Dalton Trans.* **2005**, 3331.
 (32) (a) Roesky, H. W.; Noltemeyer, M.; Lappert, M. F.; Schmidt, H.-G.; Hao, H. *Organometallics* **1999**, *18*, 2256. (b) Waeztsada, S. D.; Liu, F.-Q.; Murphy, E. F.; Roesky, H. W.; Teichert, M.; Usón, I.; Schmidt, H.-G.; Albers, T.; Parisini, E.; Moltemeyer, M. *Organometallics* **1997**, *16*, 1260. (c) Schnitter, C.; Klimek, K.; Roesky, H. W.; Albers, T.; Schmidt, H.-G.; Röpken, C.; Parisini, E. *Organometallics* **1998**, *17*, 2249.
 (33) (a) Panisch, R.; Bolte, M.; Müller, T. *J. Am. Chem. Soc.* **2006**, *128*, 9676. (b) Tamao, K.; Hayashi, T.; Ito, Y.; Shiro, M. *J. Am. Chem. Soc.* **1990**, *112*, 2422. (c) Tamao, K.; Hayashi, T.; Ito, Y.; Shiro, M. *J. Organometallics* **1992**, *11*, 20099.
 (34) Meddour, A.; Mercier, F.; Martins, J. C.; Gielen, M.; Biesemans, M.; Willem, R. *Inorg. Chem.* **1997**, *36*, 5712.
 (35) (a) Wiberg, K. B.; Zilm, K. W. *J. Org. Chem.* **2001**, *66*, 2809. (b) Lambert, J. B.; Mazzola, E. P. *Nuclear Magnetic Resonance Spectroscopy: An Introduction to Principles, Applications, and Experimental Methods*; Pearson Education, Inc.: Upper Saddle River, NJ, 2004; pp 79–81.

lacycles that bring two reactive, coordinatively unsaturated metals into proximity results in bimetallic activation of BF_4^- to yield the observed fluoride-bridged dimers. Once this feature of the arene-linked ligands was realized in the heteroscorpionate ligand \mathbf{L}_{py} (see Supporting Information), we designed the more soluble and easier to prepare \mathbf{L}_m and \mathbf{L}^3 ligands that have proven amenable for the syntheses of fluoride-bridged metallacyclic compounds **1–4**. Although the fixed geometry of the ligands seems to favor monobridged complexes containing linear M–F–M bridges, the isolation of the dibridged **3** demonstrates that two fluoride ligands fit within the metallacyclic structure. The ligands \mathbf{L}_m and \mathbf{L}^3 , therefore, provide reliable templates for building cyclic dimeric units from metal cations of varying Lewis acidities and reactivities.

Acknowledgment. We are grateful for helpful discussion from Drs. Paul Ellis and Radu Semeniuc. We thank the National Science Foundation (CHE-0414239) for financial support. We also thank the Alfred P. Sloan Foundation for support of R.P.W. The Bruker CCD single crystal diffractometer was purchased using funds provided by the NSF Instrumentation for Materials Research Program through Grant No. DMR:9975623.

Supporting Information Available: Figures and discussion of the structure of $[\text{Fe}_2(\mu\text{-F})(\mu\text{-}m\text{-}[\text{C}(\text{py})(\text{pz})_2]_2\text{C}_6\text{H}_4)_2](\text{BF}_4)_3$. X-ray crystallographic files in CIF format for all structures reported. This material is available free of charge via the Internet at <http://pubs.acs.org>.

IC0613154